Journal of Chemical Health Risks

www.jchr.org

JCHR (2024) 14(6), 1851-1868 | ISSN:2251-6727

Green Synthesis of Silver Nanoparticles for Arsenic (III) Removal from Contaminated Water

Snehal Narkhede[1], Piyush Parkhey[3], Ashish Dadsena[1], Akansha Singhai[1], Enosh Phillips[1,3], Varaprasad Kolla[1], Reecha Sahu[2*]

[1]Amity Institute of Biotechnology, Amity University Chhattisgarh, India

[2]Biomedical Engineering and Bioinformatics, University Teaching Department, Chhattisgarh Swami Vivekanand Technical University, India

Formally, affiliated to Amity Institute of Biotechnology, Amity University Chhattisgarh

[3] Trinity International, New Delhi, India

[4]St. Aloysius' College (Autonomous), Jabalpur

(Received: 05 October 2024 Revised: 15 November 2024 Accepted: 21 December 2024)

KEYWORDS

Silver nanoparticles;

Heavy metal;

Adsorption;

Arsenic,

Green tea leaves

ABSTRACT:

Introduction: According to the pollution control board, India releases one of the highest concentrations of toxic heavy metals such as Arsenic (As III), a major cause of water pollution. These high concentrations of toxic metals in effluents interfere with the natural water resources, cause severe toxicological implications on the environment with a dramatic impact on human health. Arsenic discharge degrades the water quality, spreading toxicity and seriously affects the photosynthesis activity in plants. Furthermore, it greatly impacts the aquatic environment because of low light penetration and insufficient oxygen consumption. Therefore, effluents must be adequately treated before discharging, increasing the significant focus on water reusability alternatives.

Objectives: To investigate the green synthesis of AgNPs and its dual activity of synthesized silver nanoparticles possess antimicrobial and heavy metal adsorption activity.

Methods: Green synthesis method for AgNPs using green tea leaves and Structural and chemical characterization of AgNPs was done via UV-visible spectroscopy, FTIR for functional group determination, XRD for crystallinity, Zeta potential for stability and FE-SEM to study surface morphology. Antimicrobial activity was performed by the well diffusion method as well as MIC was performed. Arsenic adsorption was studied using strip assay (qualitative) and ICPMS (Quantitative) analysis.

Results: The AgNPs synthesized using green tea leaves confirmed by UV-VIS peak at 410nm, FTIR peaks at 3306.1cm-1 (N-H), 2359.4cm-1 (C≡C) and 1636.3cm-1 (C=C and C=O group), XRD represents crystal structure and zeta potential is negative which represents inhibition particle aggregation as well as spherical shape confirmed by FE-SEM. The AgNPs possess significant antibacterial activity against *E. coli* (10-17.33 mm), *S. aureus* (19-26 mm), *P. aeruginosa* (20.66-28.66 mm) and *E. gergoviae* (18-21.66 mm) zone of inhibition when compared with control (Tetracycline 30 mcg) with 21-37.66 mm of zone of inhibition, commonly found in contaminated water, the silver nanoparticles exhibit exceptional adsorption capacity for Arsenic ions (As III), which are often present in contaminated water and pose environmental and health risks.

Conclusions: This research highlights that AgNPs synthesized via green route can be used for wastewater treatment, offering dual functionality in antibacterial activity and Arsenic adsorption. Arsenic adsorption was studied using strip assay (qualitative) and ICPMS (Quantitative) recorded 86% arsenic removal.

Journal of Chemical Health Risks

www.jchr.org

JCHR (2024) 14(6), 1851-1868 | ISSN:2251-6727

1. INTRODUCTION

The contemporary global community grapples with a paramount challenge: environmental pollution [1] of particular concern is the proliferation of heavy metals, a primary ecological threat jeopardizing human health, as well as animal and plant life [2, 3]. Heavy metals, defined as natural elements with high atomic weight and density at least five times that of water, are essential in trace amounts but pose risks in elevated concentrations [4]. The escalation of industrialization and urbanization since the mid-20th century has intensified heavy metal accumulation in the environment, elevating their mobility and transport rates. Consequently, numerous nations have implemented stringent regulations on permissible heavy metal concentrations in wastewater, prompting extensive research into remedial strategies to comply with legal thresholds.

Water, a vital resource for sustaining life on Earth, faces escalating challenges due to burgeoning population growth and dwindling surface water resources. Groundwater, comprising a mere 30.1% of 1386 million-km^3 of total water and freshwater is 10.63 million-km^3 [5], confronts mounting pressure exacerbated by high arsenic concentrations—a pervasive global issue threatening the health of an estimated 200 million people exposed to arsenic levels exceeding WHO limits in drinking water [6]. Arsenic contamination primarily arises from various geological and anthropogenic processes, with Asia, particularly India and Bangladesh, bearing the brunt of the crisis. Arsenic exposure poses severe health risks, including neurological, cardiovascular, immunological, and carcinogenic effects. Consequently, arsenic contamination emerges as a critical agricultural and health concern worldwide due to its highly toxic and persistent nature [7]. The process which are majorly responsible for excvessive arsenic deposition is reductive dissolution of iron-containing metals [8], alkali desorption [9], geothermal activities [10], leaching and weathering of silicate and carbonate minerals [11] and crustal processes [12].

In the Earth's crust, As is ranked the 53rd most abundant element with the level of 1.5 mg/L [13, 14]. In Asia arsenic contamination is found in India and Bangladesh [15-17] leads to various disesaes like lung cancer [18], skin cancer [19], reproductive, neurological and immnunological diseases [20, 21]. The major route of Arsenic to humans is *via* the use of As-rich drinking water [22, 23].

Various treatment methods which are commonly used for heavy metal removal, including photocatalysis: is the oxidation method utilizes light energy which converts harmful pollutants into harmless with the use of phtocatalysts which accelerates chemical reactions [24], chemical precipitation: it involves addition of certain chemicals such as sodium hydroxide which reacts with metal ions and others ions which is effective in removing heavy metals from water [25], Biological strategies: here biological methods such as bacteria, fungi, algae and plants are used for heavy metal remediation, for example phytoremediation is the remediation process where plant absorbs and accumulate heavy metals from soil and water [26], ion exchange: resins or memebranes are used which selectively exchanges heavy metal ions and other ions (hydrogen and sodium ions) used for heavy metal removal from water, ultrafiltration or nanofilteration selectively remove heavy metal ions based on their size and charge and generally used in water purification systems, electrochemical treatment: it involves applying an electric current to electrodes immersed in contaminated water, leads to reduction or precipitation of heavy metals which is easy to remove, reverse osmosis: here membranes allow water molecules to pass through it rejecting dissolved ions which includes heavy metals and used for treatment of industrial wastewater, evaporation generally used to treat smaller volumes of wastewater where after evaporation residues of concentrated heavy metals are obtained and in foam flotation methods air bubbles are used for heavy metal removal from water here bubbles gets attached to heavy metals causing them to rise to the surface for removal, and adsorption is the surface phenomena where adsorbate molecules (e.g., heavy metals) adhere to the surface of an adsorbent material (e.g., nanoparticles) this process is driven by various forces such as Van der walls forces, electrostatic interactions and chemical bonding [25], have been employed to purify water contaminated with heavy metals. Among these, adsorption stands out as a burgeoning technology due to its design flexibility, ability to produce high-quality treated effluent, and renewability of adsorbents. There

Journal of Chemical Health Risks

www.jchr.org

JCHR (2024) 14(6), 1851-1868 | ISSN:2251-6727

are different nanomaterial synthesis methods reported chemical vapor deposition forms thin film or nanomaterial [27], thermal decomposition is used in the synthesis of metal oxide nanoparticles via heating, hydrothermal synthesis uses high pressure and temperature to synthesize nanomaterials (nanocrystals, nanoparticles, and quantum dots) from aqueous solutions, combustion method and microwave synthesis via microwave irradiation and sol-gel method involves the hydrolysis and condensation of metal alkoxides to form a gel which is further dried and annealed or calcinated to produce metal oxide nanomaterials [28].

Arsenic treatment methods reported till date are Ion exchange and chemical precipitation by the addition of iron or aluminium salts to arsenic contaminated water results in arsenic precipitation and can be removed by sedimentation or filteration [25], reverse osmosis or nanofilteration selectively removes arsenic ions based on their size and charge which results in producing high quality water [29], Bioremediation process where microorganisms convert arsenic to less toxic forms or immobilize it in soils or sediments which is manageable [30], Adsorption process where activated carbon, graphene oxide and silica nanoparticles are used to bind and remove arsenic ions from water. This method is generally used due to its high surface area and affinity of these materials for arsenic [31].

Recently nanomaterials have gathered significant attention for their potential in heavy metal removal due to their unique properties. Graphene oxide is a nanomaterial with high surface area which enables it to adsorb heavy metal ions effectively, this capability is attributed to its functional groups and large surface-to-volume ratio [32], metal oxide nanoparticles such as iron oxide, mangenase oxide and zinc oxide have been explored for heavy metal removal, they adsorb metal ions through surface interactions, Silica and Titanium oxide nanoparticles are reported for their tunable surface properties and can be functionalizes for selective heavy metal adsorption generally used in water treatment processes and photocatalytic activity allows to degrade organic pollutants and adsorb heavy metals under UV exposure [33]. Researchers have explored a range of adsorbents, such as carbon nanomaterials which is the combination of activated carbon [34-37] and carbon nanotubes are generally used due to their tubular structure and large surface area [33, 38-42], zeolites [43-46], fullerenes and graphenes [47-52] and nanomaterials [53, 54] to extract heavy metal ions from industrial wastewater. Notably, nanomaterials are increasingly favored for their unique properties, including low toxicity, stability, large pore size, and significant specific surface area conducive to high adsorption capacity. For instance, Li et al. demonstrated the efficient removal of copper from aqueous solutions, achieving a remarkable 99% efficiency even in the presence of other metals. This underscores the efficacy of adsorption-based methods in addressing heavy metal contamination in wastewater derived from industrial processes [55]. Nanoparticles are materials with the dimensions in the nanometer scale (1-100 nm), exhibiting unique physical, chemical, and biological properties due to their particle size, surface reactivity, charge, high surface area, and quantum effects. Different types of nanoparticles reported such as silver, titanium, cerium, gold, zinc, platinum, silica and many more. There are various methods of synthesis such as top-down approaches including high energy ball milling, physical vapor deposition, laser and flash spray pyrolysis and bottom-up approaches including sol-gel method, precipitation, hydrothermal, thermal decomposition methods.

Silver nanoparticles (AgNPs) emerge as a promising solution due to the presence of several properties that make them perfect candidate for heavy metal adsorption such as simple synthesis, high surface area due to their nanoscale size. The increased surface area allows more interactions with the heavy metals which enhances adsorption efficiency and agnps exhibit strong adsorption capabilities results in removing heavy metal ions from water, they also have unique electronic properties and biocompatibility [56], morphology and adaptability [57], for combating microbial threats owing to their antimicrobial properties and low toxicity. Silver nanoparticles also possess antimicrobial activity which is the advantage and hence are used in water treatment. They can inhibit bacterial growth and prevents biofouling on surfaces. They can act as catalysts in various reactions and helps in heavy metals removal. They exhibit unique optical properties which helps in colorometric detection of heavy metal ions. They also remain stable at different temperatures and environmental conditions during water treatment [58].

Journal of Chemical Health Risks

www.jchr.org

JCHR (2024) 14(6), 1851-1868 | ISSN:2251-6727

These nanoparticles exhibit enhanced antibacterial activity compared to pure silver metal, attributed to their high surface-to-volume ratio facilitating interactions with microbial cell walls [59]. The mechanisms underlying AgNP-microorganism interactions remain incompletely understood, although proposed mechanisms include disruption of cell wall and cell permeability leads to leakage of cell [60, 61], inactivation of proteins due to interference of AgNPs and leads to DNA damage [62], and the release of reactive oxygen species due to Ag^+ ions and ATP production disturbance [63].

Green tea leaves (*Camellia sinensis L.*) are a prominent plant source of polyphenols [64]. The location, growing method, meteorological circumstances, and harvesting time all have a considerable impact on chemical makeup. Green tea leaves contain a variety of bioactive compounds, including carbohydrates, amino acids, proteins, pigments and minerals. Polyphenols, namely epicatechin gallate, epicatechin, epigallocatechin, and epigallocatechin gallate [65-68], are the predominant chemical component of dried leaves, accounting for up to 30% of their mass. Green tea extracts have been shown to effectively synthesize silver nanoparticles in prior studies [69-71]. AgNPs derived from extracts were tested for antibacterial and antifungal properties [72-79].

In this study, silver nanoparticles were synthesized using green tea extracts processed through sol-gel method, leveraging their rich phytochemical constituents for metallic ion reduction. Characterization of the synthesized AgNPs involved UV-vis spectrometry, FTIR analysis for functional groups, and scanning electron microscopy (FE-SEM) for morphology. The antibacterial activity of the synthesized AgNPs was evaluated alongside arsenic and chromium adsorption, demonstrating the potential multifunctionality of green tea-based nanoparticles in environmental remediation.

2. OBJECTIVES

To synthesize silver nanoparticles via the green route and to study its dual activity.

3. EXPERIMENTAL PROCEDURE

Materials

Silver nitrate, Hi-LR ($AgNO_3$) was purchased from Himedia, Mumbai, and Sodium Hydroxide Pellets 98% (NaOH) were purchased from Loba Chemie Pvt. Ltd., Mumbai were used further without any purification. Milli Q water was used throughout the experiments. *Camellia sinensis* leaves was purchased from Ty-phoo, Apeejay Tea Limited, Kolkata, India.

Preparation of green tea leaf extract

The aqueous extract of *C. sinensis* was prepared by taking 1.0 g of dried leaves were poured into a 250 mL beaker containing 100 mL of Milli Q water. The beaker was kept in the water bath at 40℃ for 15-20 minutes. The mixture was cooled and filtered using Whatman No. 1 filter paper. The aqueous leaf extract of *C. sinensis* was used for the synthesis of silver nanoparticles (AgNPs) and the rest of the filtered extract was stored in a screw cap bottle, in a cool environment and dry place for further use as displayed in Figure 1A.

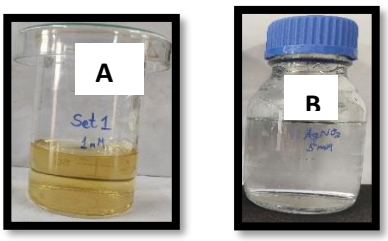

Figure 1. A represents green tea leaves extract and B represents 5mM silver nitrate solution

Synthesis of silver nanoparticles via Camellia sinensis leaves extract

0.107 g of silver nitrate powder was added in 100 ml of Milli Q water with continuous stirring till we obtained a homogenous solution for 1mM and for 5mM 0.535 g of silver nitrate in 100 ml of Milli Q water and store for further use as shown in Figure 1B.

Journal of Chemical Health Risks

www.jchr.org

JCHR (2024) 14(6), 1851-1868 | ISSN:2251-6727

To initiate the synthesis of AgNPs 40 mL aqueous green tea leaf extract was mixed with 10 mL of aqueous silver nitrate solution under continuous stirring at 200 rpm at room temperature for one hour, the color of the reaction mixture started to turn light yellow with the addition of 0.1 M NaOH so that the pH of solution shift towards alkaline, pH high enhanced the nucleation rate. After half an hour the mixture was kept in the water bath at 60℃ for 10-15 minutes and the color change to dark brown as shown in Figure 2.

The experimental solution was cooled, and the final product was collected by centrifuging the reaction mixture at 10000 rpm for 30 minutes. The pellet was washed two times with MilliQ water and washed two times with methanol, to remove any additional impurities or unreacted materials. The pellet was kept in a hot air oven at 100℃ for 1-2 h for complete dryness. Scrap the nanoparticles using a glass slide crush them till powdered form and store them in a vial for further use. The method was optimized using the protocol by Asghar et al., [70].

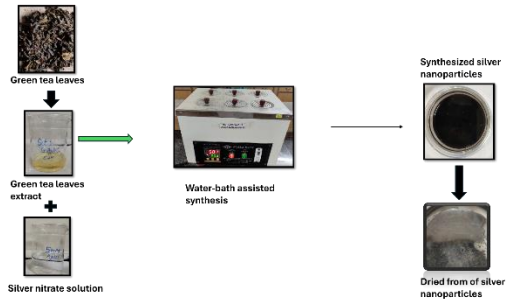

Figure 2. Green synthesis routes of silver nanoparticles using green tea leaves

Characterization of synthesized silver nanoparticles

Spectrophotometric analysis (UV-Visible)

The UV spectra were used to ascertain the formation of AgNPs. The UV-Visible absorption spectrum of the synthesized silver nanoparticles was scanned in the wavelength range of 300-600 nm by using DeNovix DS-11 spectrophotometer. The maximum absorbance of the synthesized silver nanoparticles was recorded [80].

Fourier Transform Infrared spectrum analysis (FTIR)

The IR spectra of the centrifuged green tea AgNPs were used to identify functional groups present and involved in the synthesis and capping of green tea AgNPs. The FTIR spectra were recorded using Benchtop Lt4100 Labtronics. The spectra were read at a resolution of 4 cm^{-1} within the range of 400-4000 cm^{-1}. The FTIR analysis was performed at Agilent Technologies Mumbai, Maharashtra, India [80].

X-Ray Diffraction analysis (XRD)

The synthesized silver nanoparticles were studied using XRD analysis to understand the crystalline structure. The X-Ray Diffractometer (Phillips Diffractometer 3200) equipped with a Cu Kα radiation source (1.5418) set at 40KV and 30 mA scanned the samples at a step size of 3°, between the grade range (2Θ) 10° to 80° [81].

Zeta potential analysis

The Zeta potential of synthesized silver nanoparticles was performed for the particles charge and stability using Nicomp Nano Z3000 Zeta potential Analyzer with the range of 200 to -200 mV. The Zeta potential analysis was performed at Anton Paar Mumbai, India [82].

Field Emission Scanning Electron Microscopic analysis (FE-SEM)

FE-SEM was used to characterize the morphology and particle size of AgNPs. The FE-SEM imaging of the synthesized silver nanoparticles was scanned using scanning electron microscopy Model number EM 30 Analytical Technologies SEM-3000 with different resolution range of 400 µm and 100 nm. The samples were analyzed at Mumbai, Maharashtra, India [83, 70].

Antibacterial bacterial activity of synthesized silver nanoparticles

Minimum Inhibitory Concentration

To determine the concentration range of silver nanoparticles that inhibit bacterial growth, a stock solution of nanoparticles was diluted in sterile media. A fresh culture of *Escherichia coli*, *Staphylococcus aureus*, *Pseudomonas aeruginosa* and *Enterobacter*

Journal of Chemical Health Risks

www.jchr.org

JCHR (2024) 14(6), 1851-1868 | ISSN:2251-6727

gergoviae and was standardized to 0.5 McFarland standards having a desired cell density. In separate tubes, (Luria Bertini) LB broth (10 ml) different concentrations of silver nanoparticles (50-500 µg) were added along with the standard bacterial culture. The tubes were incubated at 37℃ for 18 hours at 320 rpm in rotary shaker incubator. The presence or absence of visible bacterial growth was then determined by examining the turbidity of the broth solution and the OD was recorded at 600 nm using UV-visible spectroscopy with slight modifications in the protocol [84, 85].

Well diffusion method

The inhibition of bacterial growth of green tea AgNPs was carried out by the well diffusion method. Bacterial species such as *Escherichia coli*, *Staphylococcus aureus*, *Pseudomonas aeruginosa* and *Enterobacter gergoviae* were used for the present study.

One day before the study, 5 ml of nutrient broth was allowed to get inoculated by the pure culture which was incubated at 37℃ for 24 hours. Once the growth was observed in the nutrient broth it was set for a particular optical density by considering McFarland turbidity standard. Here O.D. at 0.5 was considered and set for inoculation. This was achieved by adding sterile nutrient water in the nutrient broth till the desired O.D. was not achieved. Further, the set 0.5 O.D. bacterial broth (10µl) was inoculated on the solidified Luria Bertani (LB) agar plates and applied throughout by a spreader further 5 minutes of diffusion time was given which allowedbfamrabfamcomplete diffusion of nutrient broth into the medium and puncture wells using cork borer in the plate. Once the broth diffuses completely place the antibiotic disc Tetracycline 30 mcg (positive control) was placed with the help of forceps and pressed gently to position them perfectly on the agar surface. Add different concentrations of silver nanoparticles in the wells such as 25 µl (25µg), 50 µl (50µg), 75 µl (75µg), and 100 µl (100µg) respectively with slight modifications in the experiment procedure [86].

Once the plates were diffused completely, all plates were incubated at 37℃ for 24 hours. After incubation time occurred zone of inhibitions in millimetres was recorded by using Himedia inhibition scale.

Heavy metal adsorption using silver nanoparticles

Qualitative analysis of Arsenic Adsorption via strip test

To perform a qualitative analysis of Arsenic adsorption using green synthesized silver nanoparticles. The silver nanoparticles (0.5g) were incubated with Arsenic contaminated solution (10 ml) for 12-24 hrs in rotary shaker incubator and then it was centrifuged at 10000 rpm for 15 minutes and the supernatant was used for the further study.

In the present study, the qualitative examination of arsenic adsorption was carried out using a Merquant test kit, which provides a visual indicator of arsenic presence in the solution. The technique began by partly inserting a test strip into the slot of the reaction vessel's top, then carefully transferring 5 ml of the solution to be tested into the vessel with a syringe. A measured teaspoon of Reagent 1 was added to the vessel, and it was shaken well. 10 drops of Reagent 2 (HCL 32%) were then added, and the jar was quickly shut. The combination was left to react for 30 minutes, with periodic gentle spinning. Following the reaction period, the test strip was withdrawn from the jar, washed quickly with water, and shaken to remove any surplus liquid. The color change in the response zone on the strip was then compared to the supplied color scale. This qualitative evaluation of the color shift was used to identify the presence of arsenic in the solution, with the intensity of the color change indicating the amount of arsenic.

Quantitative analysis of Arsenic Adsorption via (Inductively Coupled Plasma Mass Spectrometry) ICPMS analysis

The synthesized silver nanoparticles were incubated in contaminated water containing different concentrations of arsenic for 24 hours in rotary shaker incubator and the nanogels were dried and characterized for heavy metal adsorption using ICP-MS. The ICP-MS studies were performed at NEERI, Nagpur, Maharashtra, India.

4. RESULTS AND DISCUSSION

As mentioned before, colour change from pale yellow to dark brown/black is the strong indication of silver nanoparticles formation as shown in Figure 3. The

Journal of Chemical Health Risks

www.jchr.org

JCHR (2024) 14(6), 1851-1868 | ISSN:2251-6727

synthesized AgNPs was later characterized for confirmation using UV-Visible spectroscopy for surface plasmon resonance (SPR) of AgNPs, functional groups determination and surface morphology was carried by FTIR and FE-SEM, and finally the phases and crystallinity of AgNPs were characterized by XRD.

Characterization of synthesized silver nanoparticles

UV-Visible spectroscopy analysis

According to Petryayeva and Krull, [87], the optical property of synthesized AgNPs is sensitive to shape, size, concentration and aggregation state. Figure 3 represents the visual color change of light yellowish green tea ttrleaves extract into brown/black color which indicates the formation of green tea leaves silver nanoparticles. According to Sokmen et al., [72], the change in the color of the solution from pale yellow to yellowish brown or to deep brown indicates the formation of silver nanoparticles due to the excitation of surface plasmon resonance.

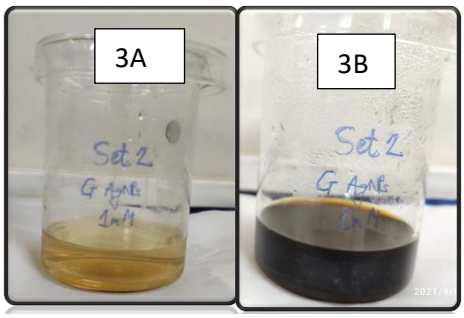

Figure 3. Preliminary conformation of green tea silver nanoparticles. (A) GT extract (B) GT AgNPs

To confirm the formation of silver nanoparticles in a colloid solution via the surface plasmon resonance phenomena of metallic nanoparticles, the UV-visible spectrophotometer is widely used. The UV scan showed a distinct Gaussian-shaped peak at 410 nm as shown in Figure 4 which confirms the formation of silver nanoparticles.

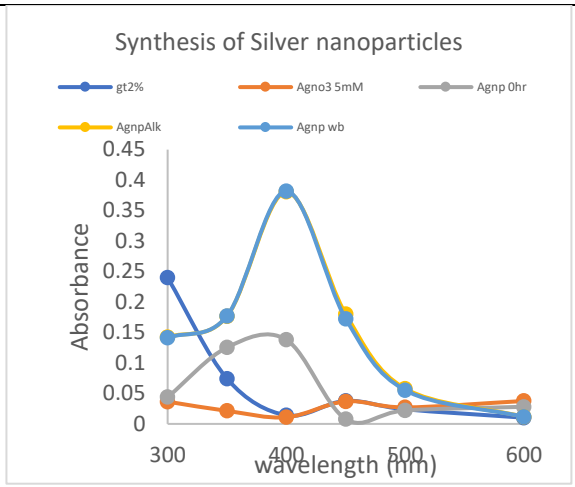

Figure 4. UV spectrum of AgNPs synthesized from green tea leaves extract

The UV scan showed a distinct Gaussian-shaped peak at 410 nm as reported by Widatalla et al., [88]. According to Rolim et al., [71], the SPR band was observed at 410 in UV-visible region. Similar study was carried out by Loo and his co-workers [89], reported that the broad absorption peak was observed at 436 nm. Kaimuangpak *et al.* [90], the absorption peak of AgNPs was observed at 450 nm due to the excitation of surface plasmon resonance.

According to Afandy et al., [80], AgNPs resonance peak is observed in the range of 400-600 nm, a broad absorption peak at 470 nm ensures the production of AgNPs. Similarly, the study carried out by Ronavari et al., [74] reported that the peak maxima was observed at 456 nm

Increasing silver nitrate concentration results in more concentrated yield of AgNPs as reported by Sokmen et al., [72]. They reported that as we increase the concentration of silver nitrate from 1 mM to 6 mM the yield of AgNPs is obtained in concentrated form.

FTIR analysis

The presence of functional groups on the surface of nanoparticles was studied through FTIR. Figure 5 and Table 1 represents the FTIR analysis of synthesized AgNPs showed distinguishing peaks at 3306.1 cm^-1, 2359.4 cm^-1 and 1636.3 cm^-1.

Journal of Chemical Health Risks

www.jchr.org

JCHR (2024) 14(6), 1851-1868 | ISSN:2251-6727

In FTIR analysis, a wavenumber of 3306.1 cm^-1 indicates the stretching vibration of an N-H bond, which is often seen in primary amines (RNH2) and amides (RCONH2). The peak at 3306.1 cm^-1 indicates the stretching vibration of the N-H bond. There is no distinct bending vibration associated with this wavenumber since stretching vibrations dominate in this range with the transmittance intensity of 43.501%.

According to Loo et al., [89], the intense broad band observed at 3271 cm $^{-1}$ was due to N-H and O-H stretching mode in the linkage of proteins. Similarly, according to Rolim et al., [71], the bands at 3440 cm^{-1} was associated with O-H stretching vibration which is assigned to -OH group of polyols such as catechins.

In FTIR analysis, a wavenumber of 2359.4 cm^-1 indicates the stretching vibration of a triple bond, particularly a carbon-carbon (C≡C) triple bond. The peak at 2359.4 cm^-1 indicates the stretching vibration of the C≡C bond. There is no distinct bending vibration associated with this wavenumber since stretching vibrations dominate in this range. Carbon-carbon triple bonds are frequent in alkynes, which are unsaturated hydrocarbons with at least one C≡C bond with intensity of 93.112 %

In FTIR analysis, a wavenumber of 1636.3 cm^-1 indicates the stretching vibration of a carbon-carbon double bond (C=C) in conjugation with a carbonyl group (C=O). This is frequently seen in compounds like ketones and aldehydes. The peak at 1636.3 cm^-1 indicates the stretching vibration of the C=C bond in conjugation with the C=O bond with transmittance intensity of 63.623% was similar to the results reported by Ronavari et al., [74] that peak at 1630 cm^{-1} was assigned to C=C vibration of aromatic structures. According to Afandy et al.,[80], the broad band at 1636 cm^{-1} represents the presence of aromatic rings and the stretching of C=O of carboxylic acid.

There is no distinct bending vibration associated with this wavenumber since stretching vibrations dominate in this range.

According to Loo et al., [89] and Rolim et al., [71], the broad peak appeared at 1637 cm^{-1} represents C=O stretching mode and 1630 cm^{-1} represents C=O vibration bond which is conjugated with ketones, quinones, esters and carboxylic acids.

According to Waditalla et al., [88] the fTIR spectra of AgNPs reported clear peaks at 3689.8, 2924.09, and 1634 corresponds to (O-H, N-H), C-H stretching and N-H bending, respectively. The other peaks at, 1238.9 represents (aromatic amine streching), 1701 represents (C=O ketone streching), 1043 represents (C-O streching) and 761.8 cm^{-1} represents (C-H bending), respectively.

According to Sokmen et al., [72], reported the broad bands observed between 1500-200 cm^{-1} prove the presence of phenolic carbonyl groups present on the compounds which are oxidised products of phenolic compounds such as catechin, during the o-strec peak appeared at 3433 and 3421 cm^{-1} contribute to O-H (Hydroxyl group), the broad peak at 2922 cm^{-1} represents C-H stretching and 1664 represents stretching vibration of C=O bond.

Table 1. FTIR peaks analysis of synthesized silver nanoparticles

Peak Number	Wavelength (cm^{-1})	Intensity borad band
1	1636.3	63.623
2	2359.4	93.112
3	3306.1	43.501

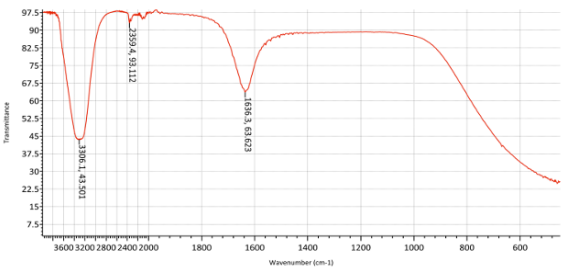

Figure 5. FTIR analysis of synthesized silver nanoparticles

XRD analysis

The XRD analysis was studied to observe the presence of crystal structure and the peaks obtained clearly show

Journal of Chemical Health Risks

www.jchr.org

JCHR (2024) 14(6), 1851-1868 | ISSN:2251-6727

the confirmatory peaks at 38.15°, 44.4°, 64.5° and 77.46° (111), (200), (220) and (311) crystal planes as shown in Figure 6.

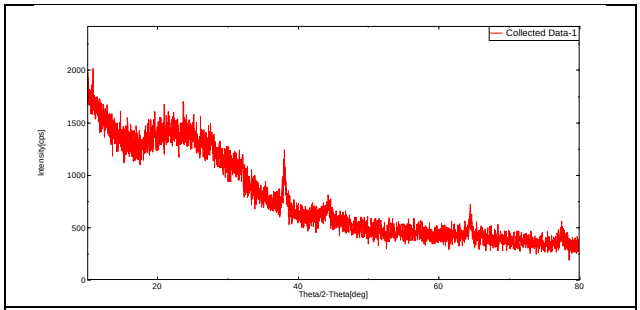

Figure 6. XRD analysis of AgNPs

According to Cavassin et al., [91] reported the XRD of AgNPs stabilized by chitosan, PVA and citrate revels the existence of the peaks at 2θ = 38.15°, 44.34°, 64.5° and 77.46°,which can be assigned to the (111), (200), (220), and (311) reflections of the face centered cubic (fcc) structure of metallic silver, respectively which is similar to our results.

Similar study was carried out by Obeid et al., [92] observe the XRD analysis exhibits the peaks at 2θ values 38.15°, 44.4°, 64.5° and 77.5°, corresponds to same planes which indicates the formation of metallic silver with face centered cubic symmetry similar to our study Alsharaeh and Othman,[93].

Zeta potential analysis

The negative zeta potential (-44.6 mV) showcased that colloidal particles are negatively charged. This negative charge can help the system maintain stability by inhibiting particle aggregation or flocculation via electrostatic repulsion.

A conductivity score of 3.259 indicates a moderate ion concentration in your colloidal system. The conductivity value can be affected by factors such as the concentration of ions from stabilizing agents or salts introduced during synthesis.

A negative electrophoretic mobility (-3.2770) indicates the direction in which negatively charged particles travel in an electric field as represented in Table 2 and Figure 7.

Table 2. Statistics table for Zeta potential

Name	Mean zeta potential [mV]	Distribution peak [mV]	Conductivity [mS/cm]	Electrophoretic Mobility [µm*cm/Vs]
Mean value	-42.0	-44.6	3.259	-3.2770
Standard deviation	1.0	1.1	0.123	0.0748
Rel. standard deviation	2.28	2.48	3.77	2.28

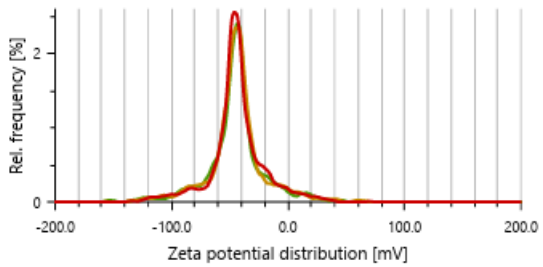

Figure 7. Zeta potential analysis of synthesized AgNPs

According to Cavassin et al., [91] the zeta potential of chitosan AgNPs possesses high positive surface charge (+41.1 mV), citrate AgNPs is negative (-48.4 mV) which is nearly similar to our study results and PVA AgNPs which is more close to zero (-17.0 mV).

According to Torabfam and Hoda, [94] and Torabfam and Yuce, [82] reported the zeta potential value of +50 mV and -17 mV which is an indicators of the electrical

Journal of Chemical Health Risks
www.jchr.org
JCHR (2024) 14(6), 1851-1868 | ISSN:2251-6727

cloud around the nanoparticles leads to high stability of the synthesizesd AgNPs.

FE-SEM analysis

The synthesized silver nanoparticles were scanned for 100 nm and 400 µm resolution and showcased spherical shape clusters with elements such as Carbon, Oxygen, Sodium, Magnesium, and Silver as represented in Figure 8.

Table 4. MIC of AgNPs

Pathogens	TET 30µg (positive control)	Negative control	50 µg	100 µg	200 µg	300 µg	400 µg	500 µg
Escherichia coli	0.134	1.675	0.167	0.154	0.158	0.148	0.131	0.121
Staphylococcus aureus	0.148	1.541	1.512	0.149	0.145	0.139	0.145	0.127
Pseudomonas aeruginosa	0.124	1.614	1.601	0.154	0.146	0.137	0.129	0.147
Enterobacter gergoviae	0.137	1.571	1.512	0.148	0.137	0.134	0.127	0.087

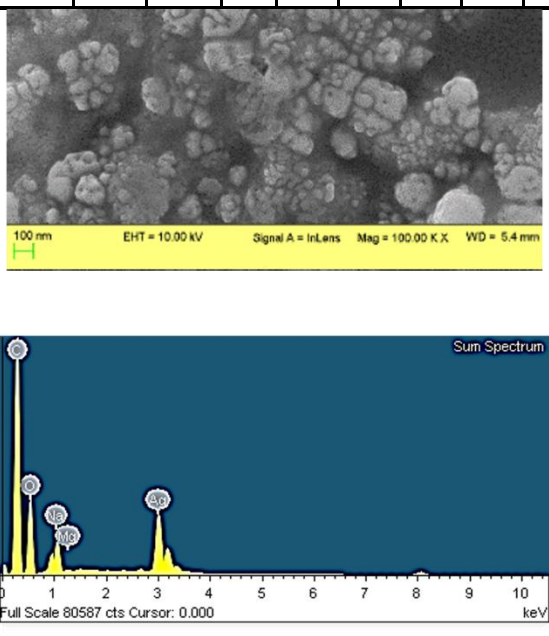

Figure 8. FE-SEM imaging of synthesized silver nanoparticles

Table 3. Elements present in the synthesized silver nanoparticles using green tea leaves extract

Element	**Weight %**	**Atomic %**
C K	50.23	63.42
O K	34.94	33.12
Na K	2.56	1.69
Mg K	0.10	0.06
Ag L	12.17	1.71
Totals	100.00	

According to Asghar et al., [70], the morphology of AgNPs synthesized using Green tea leaves showcased spherical shape with agglomeration. Similar study was carried out by Widatalla et al., [88] reported that the AgNPs are in the form of aggregates.

Antibacterial activity of silver nanoparticles

MIC of synthesized AgNPs

The synthesized silver nanoparticles were tested for Minimum Inhibitory Concentration against *Escherichia coli*, *Staphylococcus aureus*, *Pseudomonas aeruginosa* and *Enterobacter gergoviae* as shown in Table 4 and Figure 9 the MIC values observed in case of *Staphylococcus aureus*, *Pseudomonas aeruginosa* and *Enterobacter gergoviae* is 100 µg as compared to *Escherichia coli* is 200 µg.

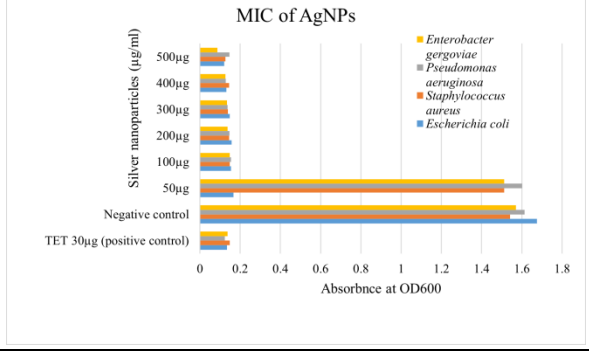

Figure 9. Graphical representation of MIC of AgNPs

According to Ahmadi et al., [95] the antibacterial activity of the synthesized AgNPs performed using 96 well plate method MIC showcased stronger activity on gram-negative bacteria as compared to gram-positive bacteria.

Journal of Chemical Health Risks

www.jchr.org

JCHR (2024) 14(6), 1851-1868 | ISSN:2251-6727

Well diffusion method of AgNPs

The antimicrobial activity of green synthesized AgNPs (25µl i.e. 75µg) against bacterial species such as *Escherichia coli*, *Staphylococcus aureus*, *Pseudomonas aeruginosa* and *Enterobacter gergoviae* when compared with control Tetracycline 30 mcg 37.66±2.08; 26.33±0.57; 28.66±0.57; and 21±1. Similarly showcased Zone of inhibition such as in 10±0; 17.66±0.57; 20.66±0.57 and 17.33±0.57 mm as shown in Table 5 and Figure 10,11.

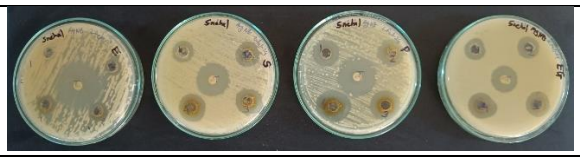

Figure 10. Antibacterial activity of silver nanoparticles against pathogens

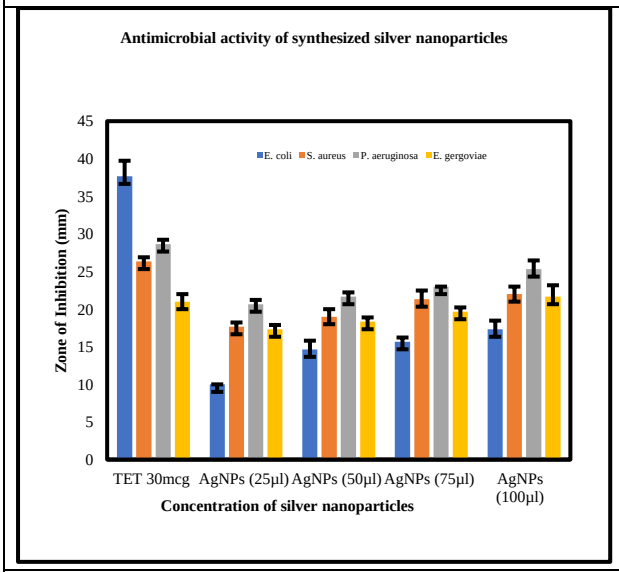

Figure 11. Graphical representation of antimicrobial activity

Similarly, when 50µl of AgNPs were added the zone of inhibition were recorded as *Escherichia coli* with 14.66±1.15, *Staphylococcus aureus* with 19±1, *Pseudomonas aeruginosa* with 21.66±0.57and *Enterobacter gergoviae* with 18.33±0.57 zone of inhibition when compared to control such as 37.66±2.08; 26.33±0.57; 28.66±0.57; and 21±1 mm.

The antimicrobial activity reported when 75µl of AgNPs were added in the well, reported zone of inhibition such as *Escherichia coli*, *Staphylococcus aureus*, *Pseudomonas aeruginosa* and *Enterobacter gergoviae*15.66±0.57; 21.33±1.15; 23±0 and19.66±0.57 mm.

Similarly, when 100µl of AgNPs were added the zone of inhibition were recorded as 17.33±1.15 mm zone of inhibition with *Escherichia coli*, 22±1 mm zone with *Staphylococcus aureus*, *Pseudomonas aeruginosa* with 25.33±1.15 mm and *Enterobacter gergoviae* with 21.66±1.52 mm zone of inhibition when compared to control such as 37.66±2.08; 26.33±0.57; 28.66±0.57; and 21±1 mm as shown in Table 5 and Figure 10,11.

Table 5. Antibacterial activity of silver nanoparticles against pathogens

	TET 30mcg (mean±SD)	**AgNPs (25µl) mean±SD**	**AgNPs (50µl) mean±SD**	**AgNPs (75µl) mean±SD**	**AgNPs (100µl) mean±SD**
E. coli	37.66±2.08	10±0	14.66±1.15	15.66±0.57	17.33±1.15
S. aureus	26.33±0.57	17.66±0.57	19±1	21.33±1.15	22±1
P. aeruginosa	28.66±0.57	20.66±0.57	21.66±0.57	23±0	25.33±1.15
E. gergoviae	21±1	17.33±0.57	18.33±0.57	19.66±0.57	21.66±1.52

According to Afandy et al., [80], *E. coli* showcased antibacterial activity at 6.4 mg/ml and 12.8 mg/ml. It has been reported that spherical shaped AgNPs exhibit a strongest antimicrobial activity against *E. coli*, *S. aureus* and *P. aeruginosa* as compared to triangle shape [96]. Similar study was conducted by Ali et al., 2022 [97] reported the antimicrobial activity of AgNPs against *E. coli*, *S. aureus* and *K. pneumoniae.*

According to Widatalla et al., [88], reported antimicrobial activity against *S. aureus* and *Klebsiella sp*. Recorded the 8-11 mm zone of inhibition when compared to our study show less zone of inhibition. One study, conducted by Asghar et al., [70], reported antimicrobial activity of AgNPs against *S. aureus* showed 19-21 mm zone of inhibition which is similar to our research.

According to Nurkhaliza et al., 2024 [86], reported potential antibacterial agents against *S. aureus* with 10±1 mm, *P. aeruginosa* with 9.5±0.5 mm, *B. subtilis*

Journal of Chemical Health Risks
www.jchr.org
JCHR (2024) 14(6), 1851-1868 | ISSN:2251-6727

with 9.5±0 mm and *E. coli* with no zone of inhibition respectively.

Arsenic adsorption using synthesized silver nanoparticles

When the qualitative analysis of arsenic adsorption was performed by strip test when compared with the control strip which is in white color, the AgNPs showcased that the arsenic contaminated sample which was of 3ppm after incubation with AgNPs for 24 hrs results in 0.5 ppm (color changes from dark brown to cream) as represented in Figure 12 which means there is 2.5 ppm removal using AgNPs.

To confirm the arsenic adsorption the AgNPs were processed for quantitative analysis via ICPMS as reported in Table 6 which represents 86% of arsenic removal.

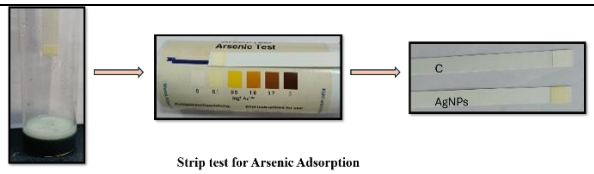

Figure 12: Qualitative analysis of Arsenic Adsorption using Strip test

Table 6. ICPMS analysis of Arsenic adsorption by green tea leaves AgNPs

Sr. No.	Sample ID	Code	Initial concentration of Arsenic (ppm) {Ci}	Arsenic on AgNPs {Cf}	Removed arsenic (ppm) {Ci-Cf}	% removal {Ci-Cf/Ci X100}
1	GT3a	Green tea AgNPs 3ppm arsenic	3	0.425 ppm	2.575	86

5. CONCLUSION

The synthesized silver nanoparticles using green tea leaves extract were characterized using UV-visible spectrophotometer, XRD, FTIR, and FE-SEM. The morphology of the synthesized silver nanoparticles using green tea leaves appears to be spherical shape in the form of aggregates. The silver nanoparticles synthesized via green route showcased antibacterial activity against selected bacterial species such as *Escherichia coli*, *Staphylococcus aureus*, *Pseudomonas aeruginosa* and *Enterobacter gergoviae*. The synthesized AgNPs also show synergistic activity with 86% of arsenic removal from contaminated water.

6. FUTURE PROSPECTS

Silver nanoparticles made from green tea leaves have bright future potential for adsorbing arsenic, providing an effective and environmentally friendly method of purifying water. By using eco-friendly plant extracts, the green synthesis approach lessens the need for hazardous chemicals and improves the nanoparticles' biocompatibility. Because of their large surface area and active adsorption sites, silver nanoparticles are useful for removing arsenic. Future studies might concentrate on incorporating these nanomaterials into scalable filtering systems, investigating regeneration strategies for nanoparticles for economical reuse, and improving synthesis conditions to increase adsorption capacity. Furthermore, research into their effectiveness in various water matrices and long-term environmental effects will be essential for real-world use.

CONFLICTS OF INTEREST

The authors have no conficts of interest to declare in this study.

ACKNOWLEDGEMENTS

Authors like to extend their sincere gratitude to Dr. Tanvir Arfin, Senior Scientist APC department, NEERI, Nagpur for the necessary support provided during ICPMS studies.

References

1. Ali, H. and Khan, E., 2017. Environmental chemistry in the twenty-first century. *Environmental Chemistry Letters*, *15*(2), pp.329-346.
2. Ali, H., Khan, E. and Sajad, M.A., 2013. Phytoremediation of heavy metals—concepts and applications. *Chemosphere*, *91*(7), pp.869-881.

Journal of Chemical Health Risks

www.jchr.org

JCHR (2024) 14(6), 1851-1868 | ISSN:2251-6727

3. Hashem, M.A., Nur-A-Tomal, M.S., Mondal, N.R. and Rahman, M.A., 2017. Hair burning and liming in tanneries is a source of pollution by arsenic, lead, zinc, manganese and iron. *Environmental Chemistry Letters*, *15*, pp.501-506.
4. Maitra, S., 2016. Study of genetic determinants of nickel and cadmium resistance in bacteria-a review. *International Journal of Current Microbiology and Applied Sciences*, *5*(11), pp.459-471.
5. Mukherjee, A., 2018. *Overview of the groundwater of South Asia* (pp. 3-20). Springer Singapore.
6. George, C.M., Sima, L., Arias, M., Mihalic, J., Cabrera, L.Z., Danz, D., Checkley, W. and Gilman, R.H., 2014. Arsenic exposure in drinking water: an unrecognized health threat in Peru. *Bulletin of the World Health Organization*, *92*, pp.565-572.
7. Chouhan, S. and Flora, S.J.S., 2010. Arsenic and fluoride: two major ground water pollutants., *Indian Journal of Experimental Biology*, 48, pp. 666–678.
8. Erbs, J.J., Berquó, T.S., Reinsch, B.C., Lowry, G.V., Banerjee, S.K. and Penn, R.L., 2010. Reductive dissolution of arsenic-bearing ferrihydrite. *Geochimica et Cosmochimica Acta*, *74*(12), pp.3382-3395.
9. Rodriguez, B.G., Rietveld, L.C., Longley, A.J. and Van Halem, D., 2019. Arsenic contamination of rural community wells in Nicaragua: a review of two decades of experience. *Science of The Total Environment*, *657*, pp.1441-1449.
10. Bundschuh, J. and Maity, J.P., 2015. Geothermal arsenic: occurrence, mobility and environmental implications. *Renewable and Sustainable Energy Reviews*, *42*, pp.1214-1222.
11. Raychowdhury, N., Mukherjee, A., Bhattacharya, P., Johannesson, K., Bundschuh, J., Sifuentes, G.B., Nordberg, E., Martin, R.A. and del Rosario Storniolo, A., 2014. Provenance and fate of arsenic and other solutes in the Chaco-Pampean Plain of the Andean foreland, Argentina: From perspectives of hydrogeochemical modeling and regional tectonic setting. *Journal of Hydrology*, *518*, pp.300-316.
12. Mukherjee, A., Verma, S., Gupta, S., Henke, K.R. and Bhattacharya, P., 2014. Influence of tectonics, sedimentation and aqueous flow cycles on the origin of global groundwater arsenic: paradigms from three continents. *Journal of Hydrology*, *518*, pp.284-299.
13. National Research Council, Division on Earth, Life Studies, Commission on Life Sciences and Safe Drinking Water Committee, 1977. Drinking Water and Health: Volume 1.
14. Sarkar, D., Datta, R. and Hannigan, R. eds., 2011. *Concepts and applications in environmental geochemistry*. Elsevier.
15. Sracek, O., Bhattacharya, P., Jacks, G., Gustafsson, J.P. and Von Brömssen, M., 2004. Behavior of arsenic and geochemical modeling of arsenic enrichment in aqueous environments. *Applied Geochemistry*, *19*(2), pp.169-180.
16. Mukherjee, A., Bhattacharya, P., Savage, K., Foster, A. and Bundschuh, J., 2008. Distribution of geogenic arsenic in hydrologic systems: controls and challenges. *Journal of Contaminant Hydrology*, *99*(1-4), pp.1-7.
17. Mukherjee, A., Bhattacharya, P. and Fryar, A.E., 2011. Arsenic and other toxic elements in surface and groundwater systems. *Applied Geochemistry*, *26*(4), pp.415-420.
18. Ferreccio Readi, C., González, C., Milosavjlevic, V., Marshall Rivera, G., Sancha, A.M. and Smith, A.H., 2000. Lung cancer and arsenic concentrations in drinking water in Chile., *Epidemiology*, 11, pp. 673–679.
19. Centeno, J.A., Tchounwou, P.B., Patlolla, A.K., Mullick, F.G., Murakata, L., Meza, E., TodorTodorov, D.L. and Yedjou, C.G., 2006. Environmental pathology and health effects of arsenic poisoning. *Managing arsenic in the environment: from soil to human health*, pp.311-327.
20. Ameer, S.S., Engström, K., Harari, F., Concha, G., Vahter, M. and Broberg, K., 2015. The effects of arsenic exposure on blood pressure and early risk markers of cardiovascular disease: evidence for population differences. *Environmental research*, *140*, pp.32-36.

Journal of Chemical Health Risks

www.jchr.org

JCHR (2024) 14(6), 1851-1868 | ISSN:2251-6727

21. Ahmad, A. and Bhattacharya, P., 2019. Environmental arsenic in a changing world. *Groundwater for Sustainable Development*, *8*, pp.169-171.
22. Shahid, M., Khalid, M., Dumat, C., Khalid, S., Niazi, N.K., Imran, M., Bibi, I., Ahmad, I., Hammad, H.M. and Tabassum, R.A., 2018. Arsenic level and risk assessment of groundwater in Vehari, Punjab Province, Pakistan. *Exposure and Health*, *10*, pp.229-239.
23. Tabassum, R.A., Shahid, M., Dumat, C., Niazi, N.K., Khalid, S., Shah, N.S., Imran, M. and Khalid, S., 2019. Health risk assessment of drinking arsenic-containing groundwater in Hasilpur, Pakistan: effect of sampling area, depth, and source. *Environmental Science and Pollution Research*, *26*, pp.20018-20029.
24. Gao, X. and Meng, X., 2021. Photocatalysis for heavy metal treatment: A review. *Processes*, *9*(10), p.1729.
25. Fu, F. and Wang, Q., 2011. Removal of heavy metal ions from wastewaters: a review. *Journal of environmental management*, *92*(3), pp.407-418.
26. Tekere, M., 2020. Biological strategies for heavy metal remediation. *Methods for bioremediation of water and wastewater pollution*, pp.393-413.
27. Hachem, K., Ansari, M.J., Saleh, R.O., Kzar, H.H., Al-Gazally, M.E., Altimari, U.S., Hussein, S.A., Mohammed, H.T., Hammid, A.T. and Kianfar, E., 2022. Methods of chemical synthesis in the synthesis of nanomaterial and nanoparticles by the chemical deposition method: a review. *BioNanoScience*, *12*(3), pp.1032-1057.
28. Khan, F.A., 2020. Synthesis of nanomaterials: methods & technology. *Applications of nanomaterials in human health*, pp.15-21.
29. Pezeshki, H., Hashemi, M. and Rajabi, S., 2023. Removal of arsenic as a potentially toxic element from drinking water by filtration: a mini review of nanofiltration and reverse osmosis techniques. *Heliyon*, *9*(3).
30. Rahman, S., Rahman, I.M. and Hasegawa, H., 2023. Management of arsenic-contaminated excavated soils: A review. *Journal of Environmental Management*, *346*, p.118943.
31. Das, P.K., Das, B.P. and Dash, P., 2021. Chromite mining pollution, environmental impact, toxicity and phytoremediation: a review. *Environmental Chemistry Letters*, *19*(2), pp.1369-1381.
32. Sontakke, A.D., Mondal, P. and Purkait, M.K., 2022. Graphene oxide-based advanced nanomaterials for environmental remediation applications. In *Advanced Nanomaterials* (pp. 155-190). Cham: Springer International Publishing.
33. Yu, G., Wang, X., Liu, J., Jiang, P., You, S., Ding, N., Guo, Q. and Lin, F., 2021. Applications of nanomaterials for heavy metal removal from water and soil: A review. *Sustainability*, *13*(2), p.713.
34. Duan, C., Ma, T., Wang, J. and Zhou, Y., 2020. Removal of heavy metals from aqueous solution using carbon-based adsorbents: A review. *Journal of Water Process Engineering*, *37*, p.101339.
35. Wong, S., Ngadi, N., Inuwa, I.M. and Hassan, O., 2018. Recent advances in applications of activated carbon from biowaste for wastewater treatment: a short review. *Journal of Cleaner Production*, *175*, pp.361-375.
36. Abbaszadeh, S., Alwi, S.R.W., Webb, C., Ghasemi, N. and Muhamad, I.I., 2016. Treatment of lead-contaminated water using activated carbon adsorbent from locally available papaya peel biowaste. *Journal of Cleaner Production*, *118*, pp.210-222.
37. Rivera-Utrilla, J., Sánchez-Polo, M., Gómez-Serrano, V., Álvarez, P.M., Alvim-Ferraz, M.C.M. and Dias, J.M., 2011. Activated carbon modifications to enhance its water treatment applications. An overview. *Journal of hazardous materials*, *187*(1-3), pp.1-23.
38. Fiyadh, S.S., AlSaadi, M.A., Jaafar, W.Z., AlOmar, M.K., Fayaed, S.S., Mohd, N.S., Hin, L.S. and El-Shafie, A., 2019. Review on heavy metal adsorption processes by carbon nanotubes. *Journal of Cleaner Production*, *230*, pp.783-793.
39. Ouni, L., Ramazani, A. and Taghavi Fardood, S., 2019. An overview of carbon nanotubes role in heavy metals removal from wastewater. *Frontiers of Chemical Science and Engineering*, *13*, pp.274-295.

Journal of Chemical Health Risks

www.jchr.org

JCHR (2024) 14(6), 1851-1868 | ISSN:2251-6727

40. Yu, G., Lu, Y., Guo, J., Patel, M., Bafana, A., Wang, X., Qiu, B., Jeffryes, C., Wei, S., Guo, Z. and Wujcik, E.K., 2018. Carbon nanotubes, graphene, and their derivatives for heavy metal removal. *Advanced Composites and Hybrid Materials*, *1*, pp.56-78.
41. Yadav, D.K. and Srivastava, S., 2017. Carbon nanotubes as adsorbent to remove heavy metal ion (Mn+ 7) in wastewater treatment. *Materials Today: Proceedings*, *4*(2), pp.4089-4094.
42. Mubarak, N.M., Sahu, J.N., Abdullah, E.C. and Jayakumar, N.S., 2014. Removal of heavy metals from wastewater using carbon nanotubes. *Separation & Purification Reviews*, *43*(4), pp.311-338.
43. Hong, M., Yu, L., Wang, Y., Zhang, J., Chen, Z., Dong, L., Zan, Q. and Li, R., 2019. Heavy metal adsorption with zeolites: The role of hierarchical pore architecture. *Chemical Engineering Journal*, *359*, pp.363-372.
44. Huang, Y., Zeng, X., Guo, L., Lan, J., Zhang, L. and Cao, D., 2018. Heavy metal ion removal of wastewater by zeolite-imidazolate frameworks. *Separation and Purification Technology*, *194*, pp.462-469.
45. Taamneh, Y. and Sharadqah, S., 2017. The removal of heavy metals from aqueous solution using natural Jordanian zeolite. *Applied Water Science*, *7*, pp.2021-2028.
46. Meng, Q., Chen, H., Lin, J., Lin, Z. and Sun, J., 2017. Zeolite A synthesized from alkaline assisted pre-activated halloysite for efficient heavy metal removal in polluted river water and industrial wastewater. *Journal of environmental sciences*, *56*, pp.254-262.
47. Yadav, J., 2018. Fullerene: Properties, synthesis and application. *Res. Rev. J. Phys*, *6*(3), pp.1-6.
48. Baby, R., Saifullah, B. and Hussein, M.Z., 2019. Carbon nanomaterials for the treatment of heavy metal-contaminated water and environmental remediation. *Nanoscale research letters*, *14*(1), p.341.
49. Nimibofa, A., Newton, E.A., Cyprain, A.Y. and Donbebe, W., 2018. Fullerenes: synthesis and applications. *J Mater Sci*, *7*, pp.22-33.
50. Sadegh, H., Ali, G.A., Gupta, V.K., Makhlouf, A.S.H., Shahryari-Ghoshekandi, R., Nadagouda, M.N., Sillanpää, M. and Megiel, E., 2017. The role of nanomaterials as effective adsorbents and their applications in wastewater treatment. *Journal of Nanostructure in Chemistry*, *7*, pp.1-14.
51. Yu, J.G., Yu, L.Y., Yang, H., Liu, Q., Chen, X.H., Jiang, X.Y., Chen, X.Q. and Jiao, F.P., 2015. Graphene nanosheets as novel adsorbents in adsorption, preconcentration and removal of gases, organic compounds and metal ions. *Science of the total environment*, *502*, pp.70-79.
52. Carpio, I.E.M., Mangadlao, J.D., Nguyen, H.N., Advincula, R.C. and Rodrigues, D.F., 2014. Graphene oxide functionalized with ethylenediamine triacetic acid for heavy metal adsorption and anti-microbial applications. *Carbon*, *77*, pp.289-301.
53. Lim, J.Y., Mubarak, N.M., Abdullah, E.C., Nizamuddin, S. and Khalid, M., 2018. Recent trends in the synthesis of graphene and graphene oxide based nanomaterials for removal of heavy metals—A review. *Journal of Industrial and Engineering Chemistry*, *66*, pp.29-44.
54. Vunain, E., Mishra, A.K. and Mamba, B.B., 2016. Dendrimers, mesoporous silicas and chitosan-based nanosorbents for the removal of heavy-metal ions: A review. *International journal of biological macromolecules*, *86*, pp.570-586.
55. Li, S., Wang, W., Liang, F. and Zhang, W.X., 2017. Heavy metal removal using nanoscale zero-valent iron (nZVI): Theory and application. *Journal of hazardous materials*, *322*, pp.163-171.
56. Sudarman, F., Shiddiq, M., Armynah, B. and Tahir, D., 2023. Silver nanoparticles (AgNPs) synthesis methods as heavy-metal sensors: A review. *International Journal of Environmental Science and Technology*, *20*(8), pp.9351-9368.
57. Dada, A.O., Adekola, F.A., Adeyemi, O.S., Bello, O.M., Oluwaseun, A.C., Awakan, O.J. and Grace, F.A.A., 2018. Exploring the effect of operational factors and characterization imperative to the synthesis of silver nanoparticles. In *Silver Nanoparticles-Fabrication, Characterization and Applications*. .IntechOpen, pp. 165–184.

Journal of Chemical Health Risks

www.jchr.org

JCHR (2024) 14(6), 1851-1868 | ISSN:2251-6727

58. Khan, M.D., Singh, A., Khan, M.Z., Tabraiz, S. and Sheikh, J., 2023. Current perspectives, recent advancements, and efficiencies of various dye-containing wastewater treatment technologies. *Journal of Water Process Engineering*, *53*, p.103579.
59. Prabu, H.J. and Johnson, I., 2015. Antibacterial activity of silver nanoparticles synthesized from plant leaf extract of Cycas circinalis, Ficus amplissima, Commelina benghalensis and Lippia nodiflora leaves., *Journal of Chemical and Pharmaceutical Research*, 7, pp. 443–449.
60. Siddiqi, K.S., Husen, A. and Rao, R.A., 2018. A review on biosynthesis of silver nanoparticles and their biocidal properties. *Journal of nanobiotechnology*, *16*, pp.1-28.
61. Kambale, E.K., Nkanga, C.I., Mutonkole, B.P.I., Bapolisi, A.M., Tassa, D.O., Liesse, J.M.I., Krause, R.W. and Memvanga, P.B., 2020. Green synthesis of antimicrobial silver nanoparticles using aqueous leaf extracts from three Congolese plant species (Brillantaisia patula, Crossopteryx febrifuga and Senna siamea). *Heliyon*, *6*(8).
62. Vijayan, R., Joseph, S. and Mathew, B., 2018. Green synthesis, characterization and applications of noble metal nanoparticles using Myxopyrum serratulum AW Hill leaf extract. *BioNanoScience*, *8*, pp.105-117.
63. Liao, C., Li, Y. and Tjong, S.C., 2019. Bactericidal and cytotoxic properties of silver nanoparticles. *International journal of molecular sciences*, *20*(2), p.449.
64. Braschi, A., Lo Presti, R., Abrignani, M.G., Abrignani, V. and Traina, M., 2023. Effects of green tea catechins and exercise training on body composition parameters. *International Journal of Food Sciences and Nutrition*, *74*(1), pp.3-21.
65. Manning, J. and Roberts, J.C., 2003. Analysis of catechin content of commercial green tea products. *Journal of Herbal Pharmacotherapy*, *3*(3), pp.19-32.
66. Das, P.R. and Eun, J.B., 2018. A comparative study of ultra-sonication and agitation extraction techniques on bioactive metabolites of green tea extract. *Food Chemistry*, *253*, pp.22-29.
67. Xu, Y.Q., Ji, W.B., Yu, P., Chen, J.X., Wang, F. and Yin, J.F., 2018. Effect of extraction methods on the chemical components and taste quality of green tea extract. *Food chemistry*, *248*, pp.146-154.
68. Lee, L.S., Kim, S.H., Kim, Y.B. and Kim, Y.C., 2014. Quantitative analysis of major constituents in green tea with different plucking periods and their antioxidant activity. *Molecules*, *19*(7), pp.9173-9186.
69. Ahmed, S., Ahmad, M., Swami, B.L. and Ikram, S., 2016. A review on plants extract mediated synthesis of silver nanoparticles for antimicrobial applications: a green expertise. *Journal of advanced research*, *7*(1), pp.17-28.
70. Asghar, M.A., Zahir, E., Shahid, S.M., Khan, M.N., Asghar, M.A., Iqbal, J. and Walker, G., 2018. Iron, copper and silver nanoparticles: Green synthesis using green and black tea leaves extracts and evaluation of antibacterial, antifungal and aflatoxin B1 adsorption activity. *Lwt*, *90*, pp.98-107.
71. Rolim, W.R., Pelegrino, M.T., de Araújo Lima, B., Ferraz, L.S., Costa, F.N., Bernardes, J.S., Rodigues, T., Brocchi, M. and Seabra, A.B., 2019. Green tea extract mediated biogenic synthesis of silver nanoparticles: Characterization, cytotoxicity evaluation and antibacterial activity. *Applied Surface Science*, *463*, pp.66-74.
72. Sökmen, M., Alomar, S.Y., Albay, C. and Serdar, G., 2017. Microwave assisted production of silver nanoparticles using green tea extracts. *Journal of Alloys and Compounds*, *725*, pp.190-198.
73. Rajput, D., Paul, S. and Gupta, A., 2020. Green synthesis of silver nanoparticles using waste tea Leaves. *Advanced Nano Research*, *3*(1), pp.1-14.
74. Rónavári, A., Kovács, D., Igaz, N., Vágvölgyi, C., Boros, I.M., Kónya, Z., Pfeiffer, I. and Kiricsi, M., 2017. Biological activity of green-synthesized silver nanoparticles depends on the applied natural extracts: a comprehensive study. *International journal of nanomedicine*, pp.871-883.
75. Prema, P., Veeramanikandan, V., Rameshkumar, K., Gatasheh, M.K., Hatamleh, A.A., Balasubramani, R. and Balaji, P., 2022. Statistical optimization of silver nanoparticle synthesis by green tea extract and its efficacy on colorimetric

detection of mercury from industrial waste water. *Environmental Research*, *204*, p.111915.

76. Babu, S., Claville, M.O. and Ghebreyessus, K., 2015. Rapid synthesis of highly stable silver nanoparticles and its application for colourimetric sensing of cysteine. *Journal of Experimental Nanoscience*, *10*(16), pp.1242-1255.
77. Sun, Q., Cai, X., Li, J., Zheng, M., Chen, Z. and Yu, C.P., 2014. Green synthesis of silver nanoparticles using tea leaf extract and evaluation of their stability and antibacterial activity. *Colloids and surfaces A: Physicochemical and Engineering aspects*, *444*, pp.226-231.
78. Chandra, A., Bhattarai, A., Yadav, A.K., Adhikari, J., Singh, M. and Giri, B., 2020. Green synthesis of silver nanoparticles using tea leaves from three different elevations. *ChemistrySelect*, *5*(14), pp.4239-4246.
79. Bergal, A., Matar, G.H. and Andaç, M., 2022. Olive and green tea leaf extracts mediated green synthesis of silver nanoparticles (AgNPs): comparison investigation on characterizations and antibacterial activity. *BioNanoScience*, *12*(2), pp.307-321.
80. Hassan Afandy, H., Sabir, D.K. and Aziz, S.B., 2023. Antibacterial activity of the green synthesized plasmonic silver nanoparticles with crystalline structure against gram-positive and gram-negative bacteria. *Nanomaterials*, *13*(8), p.1327.
81. Asif, M., Yasmin, R., Asif, R., Ambreen, A., Mustafa, M. and Umbreen, S., 2022. Green synthesis of silver nanoparticles (AgNPs), structural characterization, and their antibacterial potential. *Dose-Response*, *20*(2), p.15593258221088709.
82. Torabfam, M. and Yüce, M., 2020. Microwave-assisted green synthesis of silver nanoparticles using dried extracts of Chlorella vulgaris and antibacterial activity studies. *Green Processing and Synthesis*, *9*(1), pp.283-293.
83. Eyssa, H.M., Afifi, M. and Moustafa, H., 2023. Improvement of the acoustic and mechanical properties of sponge ethylene propylene diene rubber/carbon nanotube composites crosslinked by subsequent sulfur and electron beam irradiation. *Polymer International*, *72*(1), pp.87-98.
84. Gahlaut, A., Dabur, R. and Chhillar, A.K., 2013. Anti-Aspergillus activity of selected medicinal plants. *journal of pharmacy research*, *6*(4), pp.419-422.
85. Karuppusamy, S. and Rajasekaran, K.M., 2009. High throughput antibacterial screening of plant extracts by resazurin redox with special reference to medicinal plants of Western Ghats. *Global Journal of Pharmacology*, *3*(2), pp.63-68.
86. Nurkhaliza, F., Risana, M.Z., Pubasari, A., Priatmoko, S., Prastya, M.E. and Andreani, A.S., 2024. Comparative study of well diffusion and disc diffusion method to investigate the antibacterial properties of silver nanoparticles synthesized from Curcuma longa extracts. In *E3S Web of Conferences* (Vol. 503, p. 09003). EDP Sciences.
87. Petryayeva, E. and Krull, U.J., 2011. Localized surface plasmon resonance: Nanostructures, bioassays and biosensing—A review. *Analytica chimica acta*, *706*(1), pp.8-24.
88. Widatalla, H.A., Yassin, L.F., Alrasheid, A.A., Ahmed, S.A.R., Widdatallah, M.O., Eltilib, S.H. and Mohamed, A.A., 2022. Green synthesis of silver nanoparticles using green tea leaf extract, characterization and evaluation of antimicrobial activity. *Nanoscale Advances*, *4*(3), pp.911-915.
89. Loo, Y.Y., Chieng, B.W., Nishibuchi, M. and Radu, S., 2012. Synthesis of silver nanoparticles by using tea leaf extract from Camellia sinensis. *International journal of nanomedicine*, pp.4263-4267.
90. Kaimuangpak, K., Tamprasit, K., Date, A., Wongwiwatthananukit, S., Chang, L.C. and Weerapreeyakul, N., 2023. Synthesis of bioactive spherical silver nanoparticles with surface plasmon resonance using ethanolic twig extract of Cratoxylum formosum ssp. pruniflorum. *Journal of Drug Delivery Science and Technology*, *88*, p.104897.
91. Cavassin, E.D., de Figueiredo, L.F.P., Otoch, J.P., Seckler, M.M., de Oliveira, R.A., Franco, F.F., Marangoni, V.S., Zucolotto, V., Levin, A.S.S. and Costa, S.F., 2015. Comparison of methods to detect the in vitro activity of silver nanoparticles

(AgNP) against multidrug resistant bacteria. *Journal of nanobiotechnology*, *13*, pp.1-16.

92. Obeid, M.M., Edrees, S.J. and Shukur, M.M., 2018. Synthesis and characterization of pure and cobalt doped magnesium oxide nanoparticles: Insight from experimental and theoretical investigation. *Superlattices and Microstructures*, *122*, pp.124-139.
93. Alsharaeh, E.H. and Othman, A.A., 2014. Microwave irradiation synthesis and characterization of RGO-AgNPs/polystyrene nanocomposites. *Polymer composites*, *35*(12), pp.2318-2323.
94. Torabfam, M. and Jafarizadeh-Malmiri, H., 2018. Microwave-enhanced silver nanoparticle synthesis using chitosan biopolymer: optimization of the process conditions and evaluation of their characteristics. *Green Processing and Synthesis*, *7*(6), pp.530-537.
95. Ahmadi, M. and Adibhesami, M., 2017. The effect of silver nanoparticles on wounds contaminated with Pseudomonas aeruginosa in mice: an experimental study. *Iranian journal of pharmaceutical research: IJPR*, *16*(2), p.661.
96. Gao, M., Sun, L., Wang, Z. and Zhao, Y., 2013. Controlled synthesis of Ag nanoparticles with different morphologies and their antibacterial properties. *Materials Science and Engineering: C*, *33*(1), pp.397-404.
97. Ali, S.G., Jalal, M., Ahmad, H., Sharma, D., Ahmad, A., Umar, K. and Khan, H.M., 2022. Green synthesis of silver nanoparticles from Camellia sinensis and its antimicrobial and antibiofilm effect against clinical isolates. *Materials*, *15*(19), p.6978.